

The gradient flow formulation of the electroweak Hamiltonian

Fabian Lange^{a,b,*}

^a*Institut für Theoretische Teilchenphysik, Karlsruhe Institute of Technology (KIT),
Wolfgang-Gaede-Straße 1, 76128 Karlsruhe, Germany*

^b*Institut für Astroteilchenphysik, Karlsruhe Institute of Technology (KIT),
Hermann-von-Helmholtz-Platz 1, 76344 Eggenstein-Leopoldshafen, Germany*

E-mail: fabian.lange@kit.edu

Flavor observables are usually computed with the help of the electroweak Hamiltonian which separates the short-distance from the long-distance regime. The Wilson coefficients are calculated perturbatively, while matrix elements of the operators require non-perturbative treatment for many processes, e.g. through lattice simulations. The resulting necessity to compute the transformation between the different renormalization schemes in the two calculations constitutes an important source of uncertainties. An elegant solution to this problem is provided by the gradient-flow formalism, already widely used in lattice simulations, because its composite operators do not require renormalization. In this contribution we report on the construction of the electroweak Hamiltonian in the gradient-flow formalism through NNLO in QCD.

*Loops and Legs in Quantum Field Theory - LL2022,
25-30 April, 2022
Ettal, Germany*

*Speaker

1. Introduction

The effective electroweak Hamiltonian is often used to compute predictions for flavor observables because it separates the short-distance from the long-distance contributions. For many processes the latter are non-perturbative. The Wilson coefficients are then usually computed within perturbation theory, while the non-perturbative matrix elements of the effective operators are computed via lattice simulations or sum rules. However, to combine both ingredients to a physical prediction, the different schemes used in the individual calculations have to be matched, which constitutes an important source of uncertainties.

The gradient-flow formalism (GFF) [1–3] offers a promising solution to this problem because flowed operators are ultraviolet (UV)-finite. Thus, the flowed operators can be used both in perturbative calculations as well as in lattice simulations. The matching between the regular and the flowed operators is perturbative and can be absorbed into flow-time dependent Wilson coefficients. This strategy has already successfully been applied to the energy-momentum tensor of QCD through next-to-next-to-leading order (NNLO) [4–6], which led to competitive thermodynamical results, see e.g. Refs. [7–10]. Furthermore, the matching matrix has also been calculated for quark-dipole operators through next-to-leading order (NLO) QCD [11, 12] and for hadronic vacuum polarization through NNLO QCD [13].

For the effective electroweak Hamiltonian the matching matrix for the current-current operators has been calculated at NLO QCD in the $\overline{\text{DR}}$ scheme in Ref. [14]. In this contribution we report on our recent calculation [15, 16] of the same matching matrix through NNLO in the basis defined in Ref. [17] which allows us to adopt the $\overline{\text{MS}}$ scheme with a fully anti-commuting γ_5 . Our result could directly be applied to predict K - or B -mixing parameters on the basis of the GFF once the corresponding matrix elements from lattice simulations become available.

2. Operator basis

Schematically the effective electroweak Hamiltonian can be written as

$$\mathcal{H}_{\text{eff}} = - \left(\frac{4G_F}{\sqrt{2}} \right)^x V_{\text{CKM}} \sum_n C_n O_n \quad (1)$$

where G_F denotes the Fermi constant raised to some power x , V_{CKM} comprises the relevant elements of the Cabbibo-Kobayashi-Maskawa (CKM) matrix, and C_n are the Wilson coefficients. As a first step we focus on the current-current operators

$$\begin{aligned} O_1 &= - \left(\bar{\psi}_1 \gamma_\mu^L T^a \psi_2 \right) \left(\bar{\psi}_3 \gamma_\mu^L T^a \psi_4 \right), \\ O_2 &= \left(\bar{\psi}_1 \gamma_\mu^L \psi_2 \right) \left(\bar{\psi}_3 \gamma_\mu^L \psi_4 \right), \end{aligned} \quad (2)$$

where we choose the basis of Ref. [17]. Furthermore, we adopt the Euclidean metric and use the short-hand notation

$$\gamma_\mu^L = \gamma_\mu \frac{1 - \gamma_5}{2} \quad (3)$$

to project onto the left-handed components of the spinors. Our convention for the color generators is

$$[T^a, T^b] = f^{abc} T^c, \quad \text{Tr}(T^a T^b) = -T_R \delta^{ab}, \quad (4)$$

with the real and totally anti-symmetric structure constants f^{abc} and the trace normalization T_R . In addition to the physical operators in Eq. (2), loop corrections in dimensional regularization with $D = 4 - 2\epsilon$ introduce contributions which have to be attributed to so-called evanescent operators. Even though they vanish for $D = 4$, they mix with the physical operators at higher orders in perturbation theory [18]. We again follow Ref. [17] and choose

$$\begin{aligned} O_1^{(1)} &= -\left(\bar{\psi}_1 \gamma_{\mu\nu\rho}^L T^a \psi_2\right) \left(\bar{\psi}_3 \gamma_{\mu\nu\rho}^L T^a \psi_4\right) - 16O_1, \\ O_2^{(1)} &= \left(\bar{\psi}_1 \gamma_{\mu\nu\rho}^L \psi_2\right) \left(\bar{\psi}_3 \gamma_{\mu\nu\rho}^L \psi_4\right) - 16O_2, \\ O_1^{(2)} &= -\left(\bar{\psi}_1 \gamma_{\mu\nu\rho\sigma\tau}^L T^a \psi_2\right) \left(\bar{\psi}_3 \gamma_{\mu\nu\rho\sigma\tau}^L T^a \psi_4\right) - 20O_1^{(1)} - 256O_1, \\ O_2^{(2)} &= \left(\bar{\psi}_1 \gamma_{\mu\nu\rho\sigma\tau}^L \psi_2\right) \left(\bar{\psi}_3 \gamma_{\mu\nu\rho\sigma\tau}^L \psi_4\right) - 20O_2^{(1)} - 256O_2. \end{aligned} \quad (5)$$

as evanescent operators, where $\gamma_{\rho\mu_1\cdots\mu_n}^L \equiv \gamma_\rho^L \gamma_{\mu_1} \cdots \gamma_{\mu_n}$. We will refer to the basis defined by Eqs. (2) and (5) as the Chetyrkin-Misiak-Münz (CMM)-basis in what follows.

3. Flowed operators

In the GFF, one introduces flowed gluon and quark fields $B_\mu^a = B_\mu^a(t)$ and $\chi = \chi(t)$ as solutions of the flow equations [3, 19]

$$\begin{aligned} \partial_t B_\mu^a &= \mathcal{D}_\nu^{ab} G_{\nu\mu}^b + \kappa \mathcal{D}_\mu^{ab} \partial_\nu B_\nu^b, \\ \partial_t \chi &= \Delta \chi - \kappa \partial_\mu B_\mu^a T^a \chi, \\ \partial_t \bar{\chi} &= \bar{\chi} \overleftarrow{\Delta} + \kappa \bar{\chi} \partial_\mu B_\mu^a T^a, \end{aligned} \quad (6)$$

with the initial conditions

$$B_\mu^a(t=0) = A_\mu^a, \quad \chi(t=0) = \psi, \quad (7)$$

where A_μ^a and ψ are the regular gluon and quark fields, respectively, and

$$\begin{aligned} \mathcal{D}_\mu^{ab} &= \delta^{ab} \partial_\mu - f^{abc} B_\mu^c, \\ G_{\mu\nu}^a &= \partial_\mu B_\nu^a - \partial_\nu B_\mu^a + f^{abc} B_\mu^b B_\nu^c, \\ \Delta &= (\partial_\mu + B_\mu^a T^a)^2. \end{aligned} \quad (8)$$

The parameter κ is arbitrary and drops out of physical quantities; we will set $\kappa = 1$ in our calculation, because this choice reduces the size of the intermediate algebraic expressions.

Our practical implementation of the GFF in perturbation theory follows the strategy developed in Ref. [20] and further detailed in Ref. [21]. The QCD propagators are generalized by multiplying them with flow-time-dependent exponential functions. The flow equations are introduced on the

Lagrangian level with the help of Lagrange multiplier fields. This leads to propagators directed towards increasing flow time, the so-called “flow lines”, and integrations over the flow times of new “flowed vertices”.

These exponential functions regulate some of the UV-divergencies so that the flowed gluon field B_μ^a does not require renormalization [3, 20]. The flowed quark fields χ , on the other hand, have to be renormalized [19]. We choose the ringed scheme for which the renormalization constant \hat{Z}_χ is defined by the all-order condition

$$\begin{aligned} \hat{Z}_\chi \langle \bar{\chi} \overleftrightarrow{D} \chi \rangle_0 \Big|_{m=0} &\equiv -\frac{2n_c}{(4\pi t)^2}, \\ \overleftrightarrow{D}_\mu &= \partial_\mu - \overleftarrow{\partial}_\mu + 2B_\mu^a T^a, \end{aligned} \quad (9)$$

where $\langle \cdot \rangle_0$ denotes the vacuum expectation value (VEV) [5]. It is known through NNLO [21].

Furthermore, it was shown that composite operators constructed from flowed fields are UV finite after the renormalization of the strong coupling, the quark masses, and the flowed fields [20]. We simply define the flowed operators by replacing the spinors ψ_i by renormalized flowed spinors $\hat{Z}_\chi^{1/2} \chi_i$ in the regular operators, i.e.

$$\begin{aligned} \tilde{O}_1 &= -\hat{Z}_\chi^2 \left(\bar{\chi}_1 \gamma_\mu^L T^a \chi_2 \right) \left(\bar{\chi}_3 \gamma_\mu^L T^a \chi_4 \right), \\ \tilde{O}_2 &= \hat{Z}_\chi^2 \left(\bar{\chi}_1 \gamma_\mu^L \chi_2 \right) \left(\bar{\chi}_3 \gamma_\mu^L \chi_4 \right), \end{aligned} \quad (10)$$

and analogously for the evanescent operators. Since they are finite, one can treat them in four space-time dimensions, which also means that flowed evanescent operators vanish. By keeping them in our calculation we can check this explicitly as a welcome consistency check on our results. Let us stress that the regular evanescent operators are still needed.

4. Small-flow-time expansion

One can relate the flowed and the regular operators through the small-flow-time expansion $t \rightarrow 0$ [20]

$$\begin{pmatrix} \tilde{O}(t) \\ \tilde{E}(t) \end{pmatrix} \asymp \zeta^B(t) \begin{pmatrix} O \\ E \end{pmatrix}, \quad (11)$$

where we use the notation

$$\begin{aligned} O &= (O_1, O_2)^T \equiv (O_1^{(0)}, O_2^{(0)})^T, \\ E &= (O_1^{(1)}, O_2^{(1)}, O_1^{(2)}, O_2^{(2)})^T, \end{aligned} \quad (12)$$

and analogously for the flowed operators. Here and in what follows, the superscript “B” denotes a “bare” quantity which will undergo renormalization. Terms of $O(t)$ are neglected as indicated by the symbol \asymp . We also adopt the block-notation of Eq. (11) for matrices, e.g. for the renormalized matching matrix we write

$$\zeta(t) = \begin{pmatrix} \zeta_{OO}(t) & \zeta_{OE}(t) \\ \zeta_{EO}(t) & \zeta_{EE}(t) \end{pmatrix}, \quad (13)$$

where the 2×2 -submatrix ζ_{OO} concerns only the physical operators.

While the flowed operators on the l.h.s. of Eq. (11) are finite, the regular operators on the r.h.s. are divergent. Hence, the bare matching matrix $\zeta^B(t)$ is divergent for $D \rightarrow 4$ as well. However, one may define renormalized operators

$$\begin{pmatrix} O \\ E \end{pmatrix}^R = Z \begin{pmatrix} O \\ E \end{pmatrix} \equiv \begin{pmatrix} Z_{OO} & Z_{OE} \\ Z_{EO} & Z_{EE} \end{pmatrix} \begin{pmatrix} O \\ E \end{pmatrix} \quad (14)$$

with the corresponding renormalization matrix Z such that matrix elements of them are finite. Usually, the blocks Z_{OO} , Z_{OE} , and Z_{EE} are defined in the $\overline{\text{MS}}$ scheme. On the other hand, the block Z_{EO} is finite and chosen such that physical matrix elements $\langle \cdot \rangle$ of evanescent operators vanish to all orders in perturbation theory [18, 22, 23], i.e.

$$\langle E^R \rangle = Z_{EO} \langle O \rangle + Z_{EE} \langle E \rangle \stackrel{!}{=} O(\epsilon). \quad (15)$$

By inserting Eq. (14) into Eq. (11), we can then define the renormalized matching matrix

$$\zeta(t) = \zeta^B(t) Z^{-1} = \begin{pmatrix} \zeta_{OO}(t) & \zeta_{OE}(t) \\ \zeta_{EO}(t) & \zeta_{EE}(t) \end{pmatrix}. \quad (16)$$

Since $\langle \tilde{E}(t) \rangle = O(\epsilon)$, the renormalization condition in Eq. (15) is equivalent to

$$\zeta_{EO}(t) = O(\epsilon). \quad (17)$$

5. Calculation of the matching matrix

To compute the matching matrix $\zeta(t)$ we employ the method of projectors [24, 25]. The projectors are matrix elements

$$P_j^{(i)}[X] = \langle 0|X|i, j \rangle \Big|_{p=m=0}, \quad (18)$$

with $i \in \{0, 1, 2\}$ and $j \in \{1, 2\}$, such that

$$P_j^{(i)}[O_{j'}^{(i')}] = \delta_{ii'} \delta_{jj'}, \quad (19)$$

where we remind the reader of the unified notation for physical and evanescent operators defined in Eq. (12). In general, the projectors could also involve derivatives w.r.t. masses and/or external momenta, but this is not necessary for the set of operators considered here. By setting all external mass scales to zero in Eq. (18), it is sufficient to satisfy Eq. (19) at tree-level, because all higher perturbative orders on the l.h.s. vanish in dimensional regularization.

The external states $|i, j\rangle$ are defined to explicitly project onto left-handed spinors. Together with an anti-commuting γ_5 this eliminates all γ_5 's from the traces at any order in the calculation [17].

Applying the projectors to Eq. (11) directly yields the bare matching matrix

$$\zeta_{jj'}^{B, (ii')}(t) = P_{j'}^{(i')}[\tilde{O}_j^{(i)}(t)], \quad (20)$$

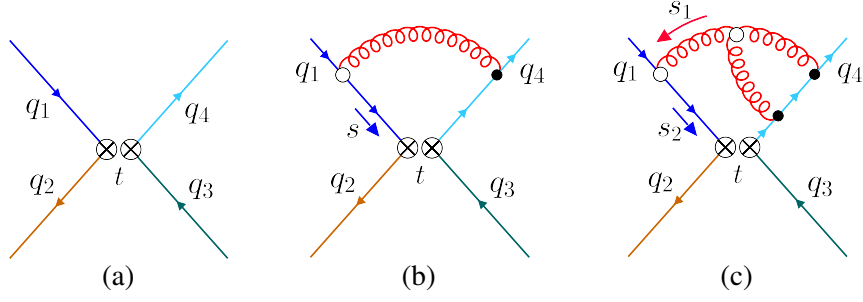


Figure 1: Sample diagrams contributing to the determination of the matching matrix $\zeta(t)$ at leading order (LO), NLO, and NNLO QCD. The circles denote “flowed vertices”, lines with an arrow next to them denote “flow lines”, and the label next to the arrow is a flow-time integration variable (see Ref. [21] for details). The diagrams were produced with FeynGame [26].

where $\zeta_{jj'}^{(00)} \equiv (\zeta_{OO})_{jj'}$. By restricting the calculation to the case with four different quark flavors in the operators, all Feynman diagrams contributing to the r.h.s. of this equation are obtained by dressing the generic tree-level diagram in Fig. 1 (a). Sample diagrams are shown in Fig. 1 (b) and (c).

The actual calculation of the diagrams is performed with the setup described in Ref. [21] based on q2e/exp [27, 28]: After generating the Feynman diagrams with qgraf [29, 30], we apply the projectors, perform the traces, and simplify the algebraic expressions within FORM [31–33]. With the help of Kira+FireFly [34–37], the resulting Feynman integrals are reduced to the same master integrals as found in Ref. [6].

6. Results

Performing the calculation and renormalization as described in the previous sections, our results for the physical components of the renormalized matching matrix through NNLO in QCD read [16]

$$\begin{aligned}
 (\zeta^{-1})_{11}(t) &= 1 + a_s \left(4.212 + \frac{1}{2} L_{\mu t} \right) + a_s^2 \left[22.72 - 0.7218 n_f + L_{\mu t} (16.45 - 0.7576 n_f) \right. \\
 &\quad \left. + L_{\mu t}^2 \left(\frac{17}{16} - \frac{1}{24} n_f \right) \right], \\
 (\zeta^{-1})_{12}(t) &= a_s \left(-\frac{5}{6} - \frac{1}{3} L_{\mu t} \right) + a_s^2 \left[-4.531 + 0.1576 n_f + L_{\mu t} \left(-3.133 + \frac{5}{54} n_f \right) \right. \\
 &\quad \left. + L_{\mu t}^2 \left(-\frac{13}{24} + \frac{1}{36} n_f \right) \right], \\
 (\zeta^{-1})_{21}(t) &= a_s \left(-\frac{15}{4} - \frac{3}{2} L_{\mu t} \right) + a_s^2 \left[-23.20 + 0.7091 n_f + L_{\mu t} \left(-15.22 + \frac{5}{12} n_f \right) \right. \\
 &\quad \left. + L_{\mu t}^2 \left(-\frac{39}{16} + \frac{1}{8} n_f \right) \right], \\
 (\zeta^{-1})_{22}(t) &= 1 + 3.712 a_s + a_s^2 \left[19.47 - 0.4334 n_f + L_{\mu t} (11.75 - 0.6187 n_f) + \frac{1}{4} L_{\mu t}^2 \right],
 \end{aligned} \tag{21}$$

with $a_s = \alpha_s(\mu)/\pi$ and $L_{\mu t} = \ln 2\mu^2 t + \gamma_E$, where α_s is the strong coupling renormalized in the $\overline{\text{MS}}$ scheme with n_f quark flavors, μ the renormalization scale, and $\gamma_E = 0.577 \dots$ Euler's constant. For the sake of compactness, we set $n_c = 3$ and $T_R = \frac{1}{2}$, and replaced transcendental coefficients by floating-point numbers. Analytical coefficients for a general $\text{SU}(n_c)$ gauge group are included in an ancillary file of Ref. [16].

The correctness of our result is supported by several observations: First of all, the renormalized matching matrix is finite when we employ the literature expression for the renormalization matrix Z from Refs. [17, 38, 39]. In addition, Eq. (17) is fulfilled with the same Z . Furthermore, our result is gauge independent even though we performed the calculation in R_ξ gauge. The final non-trivial check is the basis transformation to the so-called non-mixing basis of Ref. [40], which is defined such that the anomalous dimension matrix for the physical operators is diagonal through NNLO. In this basis the physical matching matrix $\zeta(t)$ between the $\overline{\text{MS}}$ renormalized and the flowed operators turns out to be diagonal.¹ The result in the non-mixing basis can be found in Ref. [16].

7. The effective Hamiltonian in the gradient-flow formalism

By inverting the small-flow-time expansion in Eq. (11), one can rewrite the effective electroweak Hamiltonian as

$$\mathcal{H}_{\text{eff}} \asymp - \left(\frac{4G_F}{\sqrt{2}} \right)^x V_{\text{CKM}} \sum_n \tilde{C}_n(t) \tilde{O}_n(t) \quad (22)$$

to express it in terms of the flowed operators. The flowed Wilson coefficients are given by

$$\tilde{C}_n(t) = \sum_m C_m^R \zeta_{mn}^{-1}(t), \quad (23)$$

with $\zeta(t) \equiv \zeta_{OO}(t)$ the physical part of the matching matrix, and $C_n^R = \sum_m C_m(Z^{-1})_{mn}$ the renormalized regular Wilson coefficients. Since both the flowed operators and the flowed Wilson coefficients are individually finite without operator renormalization, they are also individually scheme and renormalization scale independent (up to higher orders in perturbation theory). This is in stark contrast to C^R and O^R which depend on the renormalization scheme, including the treatment of γ_5 and the choice of evanescent operators. Eq. (22) can thus be used both perturbatively and on the lattice without matching perturbative and lattice schemes. However, on the perturbative side it is important to evaluate C^R and $\zeta^{-1}(t)$ in the same renormalization scheme.

Re-expanding the r.h.s. of Eq. (23), directly gives the flowed Wilson coefficients to the known order of either C^R or $\zeta^{-1}(t)$, whichever is lower. For Kaon mixing, i.e. $|\Delta S| = 2$, the physical operator basis from Eq. (2) reduces to just one operator due to a Fierz identity. In this case, the Standard Model (SM) Wilson coefficient is known through NLO [41], with two contributions known through NNLO [42, 43]. Similarly, only one operator contributes to the mass difference of neutral B -meson mixing, i.e. $|\Delta B| = 2$. Again, the SM Wilson coefficient is known through NLO [41]. For non-leptonic $|\Delta F| = 1$ decays, the Wilson coefficients C_m^R in the CMM basis for the SM can be found in Refs. [39, 44] through NNLO. However, we did not consider the subdominant penguin contributions in our calculation of $\zeta^{-1}(t)$ above.

¹An immediate comparison of this result to the NLO expression of Ref. [14] is not possible, because the latter is obtained in the $\overline{\text{DR}}$ scheme.

8. Conclusions and outlook

In this contribution we discussed our calculation of the matching matrix of the current-current operators of the electroweak effective Hamiltonian to their flowed counterparts through NNLO QCD published in Ref. [16]. Once the matrix elements from the lattice become available, our results can directly be applied to K - or B -meson mixing, for example. The inclusion of penguin operators for non-leptonic $|\Delta F| = 1$ decays is work in progress. It remains to be seen how the GFF approach to flavor physics compares to conventional calculations.

Acknowledgments

I thank Robert Harlander for the collaboration on this project and comments on the manuscript. Furthermore, I acknowledge financial support by the *Deutsche Forschungsgemeinschaft* (DFG, German Research Foundation) through grant 386986591 in the early stages of this project and through the Collaborative Research Centre TRR 257 funded through grant 396021762.

References

- [1] R. Narayanan and H. Neuberger, *Infinite N phase transitions in continuum Wilson loop operators*, *JHEP* **03** (2006) 064 [[hep-th/0601210](#)].
- [2] M. Lüscher, *Trivializing Maps, the Wilson Flow and the HMC Algorithm*, *Commun. Math. Phys.* **293** (2010) 899 [[0907.5491](#)].
- [3] M. Lüscher, *Properties and uses of the Wilson flow in lattice QCD*, *JHEP* **08** (2010) 071 [[1006.4518](#)].
- [4] H. Suzuki, *Energy–momentum tensor from the Yang–Mills gradient flow*, *PTEP* **2013** (2013) 083B03 [[1304.0533](#)].
- [5] H. Makino and H. Suzuki, *Lattice energy–momentum tensor from the Yang–Mills gradient flow—inclusion of fermion fields*, *PTEP* **2014** (2014) 063B02 [[1403.4772](#)].
- [6] R.V. Harlander, Y. Kluth and F. Lange, *The two-loop energy–momentum tensor within the gradient-flow formalism*, *Eur. Phys. J. C* **78** (2018) 944 [[1808.09837](#)].
- [7] T. Iritani, M. Kitazawa, H. Suzuki and H. Takaura, *Thermodynamics in quenched QCD: energy–momentum tensor with two-loop order coefficients in the gradient-flow formalism*, *PTEP* **2019** (2019) 023B02 [[1812.06444](#)].
- [8] WHOT-QCD collaboration, *$N_f = 2+1$ QCD thermodynamics with gradient flow using two-loop matching coefficients*, *Phys. Rev. D* **102** (2020) 014510 [[2005.00251](#)].
- [9] WHOT-QCD collaboration, *Latent heat and pressure gap at the first-order deconfining phase transition of $SU(3)$ Yang–Mills theory using the small flow-time expansion method*, *PTEP* **2021** (2021) 013B08 [[2011.10292](#)].

- [10] H. Suzuki and H. Takaura, $t \rightarrow 0$ extrapolation function in the small flow time expansion method for the energy–momentum tensor, *PTEP* **2021** (2021) 073B02 [[2102.02174](#)].
- [11] SYMLAT collaboration, Short flow-time coefficients of CP-violating operators, *Phys. Rev. D* **102** (2020) 034509 [[2005.04199](#)].
- [12] E. Mereghetti, C.J. Monahan, M.D. Rizik, A. Shindler and P. Stoffer, One-loop matching for quark dipole operators in a gradient-flow scheme, *JHEP* **04** (2022) 050 [[2111.11449](#)].
- [13] R.V. Harlander, F. Lange and T. Neumann, Hadronic vacuum polarization using gradient flow, *JHEP* **08** (2020) 109 [[2007.01057](#)].
- [14] A. Suzuki, Y. Taniguchi, H. Suzuki and K. Kanaya, Four quark operators for kaon bag parameter with gradient flow, *Phys. Rev. D* **102** (2020) 034508 [[2006.06999](#)].
- [15] R.V. Harlander and F. Lange, The electroweak Hamiltonian in the gradient flow formalism, *PoS EPS-HEP2021* (2022) 415 [[2110.15759](#)].
- [16] R.V. Harlander and F. Lange, Effective electroweak Hamiltonian in the gradient-flow formalism, *Phys. Rev. D* **105** (2022) L071504 [[2201.08618](#)].
- [17] K. Chetyrkin, M. Misiak and M. Münz, $||\Delta F|| = 1$ non-leptonic effective Hamiltonian in a simpler scheme, *Nucl. Phys. B* **520** (1998) 279 [[hep-ph/9711280](#)].
- [18] A.J. Buras and P.H. Weisz, QCD nonleading corrections to weak decays in dimensional regularization and 't Hooft-Veltman schemes, *Nucl. Phys. B* **333** (1990) 66.
- [19] M. Lüscher, Chiral symmetry and the Yang-Mills gradient flow, *JHEP* **04** (2013) 123 [[1302.5246](#)].
- [20] M. Lüscher and P. Weisz, Perturbative analysis of the gradient flow in non-abelian gauge theories, *JHEP* **02** (2011) 051 [[1101.0963](#)].
- [21] J. Artz, R.V. Harlander, F. Lange, T. Neumann and M. Prausa, Results and techniques for higher order calculations within the gradient-flow formalism, *JHEP* **06** (2019) 121 [[1905.00882](#)].
- [22] M.J. Dugan and B. Grinstein, On the vanishing of evanescent operators, *Phys. Lett. B* **256** (1991) 239.
- [23] S. Herrlich and U. Nierste, Evanescent operators, scheme dependences and double insertions, *Nucl. Phys. B* **455** (1995) 39 [[hep-ph/9412375](#)].
- [24] S.G. Gorishny, S.A. Larin and F.V. Tkachov, The algorithm for OPE coefficient functions in the \overline{MS} scheme, *Phys. Lett. B* **124** (1983) 217.
- [25] S.G. Gorishny and S.A. Larin, Coefficient functions of asymptotic operator expansions in the minimal subtraction scheme, *Nucl. Phys. B* **283** (1987) 452.

- [26] R.V. Harlander, S.Y. Klein and M. Lipp, *FeynGame*, *Comput. Phys. Commun.* **256** (2020) 107465 [2003.00896].
- [27] R. Harlander, T. Seidensticker and M. Steinhauser, *Complete corrections of $O(\alpha\alpha_s)$ to the decay of the Z boson into bottom quarks*, *Phys. Lett. B* **426** (1998) 125 [hep-ph/9712228].
- [28] T. Seidensticker, *Automatic application of successive asymptotic expansions of Feynman diagrams*, in *6th Conference of the ACAT series*, 1999 [hep-ph/9905298].
- [29] P. Nogueira, *Automatic Feynman Graph Generation*, *J. Comput. Phys.* **105** (1993) 279.
- [30] P. Nogueira, *Abusing qgraf*, *Nucl. Instrum. Meth. A* **559** (2006) 220.
- [31] J.A.M. Vermaseren, *New features of FORM*, [math-ph/0010025](#).
- [32] J. Kuipers, T. Ueda, J.A.M. Vermaseren and J. Vollinga, *FORM version 4.0*, *Comput. Phys. Commun.* **184** (2013) 1453 [1203.6543].
- [33] T. van Ritbergen, A.N. Schellekens and J.A.M. Vermaseren, *Group theory factors for Feynman diagrams*, *Int. J. Mod. Phys. A* **14** (1999) 41 [hep-ph/9802376].
- [34] P. Maierhöfer, J. Usovitsch and P. Uwer, *Kira—A Feynman integral reduction program*, *Comput. Phys. Commun.* **230** (2018) 99 [1705.05610].
- [35] J. Klappert, F. Lange, P. Maierhöfer and J. Usovitsch, *Integral reduction with Kira 2.0 and finite field methods*, *Comput. Phys. Commun.* **266** (2021) 108024 [2008.06494].
- [36] J. Klappert and F. Lange, *Reconstructing rational functions with FireFly*, *Comput. Phys. Commun.* **247** (2020) 106951 [1904.00009].
- [37] J. Klappert, S.Y. Klein and F. Lange, *Interpolation of dense and sparse rational functions and other improvements in FireFly*, *Comput. Phys. Commun.* **264** (2021) 107968 [2004.01463].
- [38] P. Gambino, M. Gorbahn and U. Haisch, *Anomalous dimension matrix for radiative and rare semileptonic B decays up to three loops*, *Nucl. Phys. B* **673** (2003) 238 [hep-ph/0306079].
- [39] M. Gorbahn and U. Haisch, *Effective Hamiltonian for non-leptonic $|\Delta F| = 1$ decays at NNLO in QCD*, *Nucl. Phys. B* **713** (2005) 291 [hep-ph/0411071].
- [40] A.J. Buras, M. Gorbahn, U. Haisch and U. Nierste, *Charm quark contribution to $K^+ \rightarrow \pi^+ \nu \bar{\nu}$ at next-to-next-to-leading order*, *JHEP* **11** (2006) 002 [hep-ph/0603079].
- [41] G. Buchalla, A.J. Buras and M.E. Lautenbacher, *Weak decays beyond leading logarithms*, *Rev. Mod. Phys.* **68** (1996) 1125 [hep-ph/9512380].
- [42] J. Brod and M. Gorbahn, *ϵ_K at next-to-next-to-leading order: The charm-top-quark contribution*, *Phys. Rev. D* **82** (2010) 094026 [1007.0684].
- [43] J. Brod and M. Gorbahn, *Next-to-Next-to-Leading-Order Charm-Quark Contribution to the CP Violation Parameter ϵ_K and ΔM_K* , *Phys. Rev. Lett.* **108** (2012) 121801 [1108.2036].

- [44] C. Bobeth, M. Misiak and J. Urban, *Photonic penguins at two loops and m_t -dependence of $BR[B \rightarrow X_s l^+ l^-]$* , *Nucl. Phys. B* **574** (2000) 291 [[hep-ph/9910220](#)].